1998-05-15

Tracking the Evolution of a Hydrothermal Event Plume with a RAFOS Neutrally Buoyant Drifter

Lupton, John E.

Tracking the Evolution of a Hydrothermal Event Plume with a RAFOS Neutrally Buoyant Drifter

John E. Lupton, Edward T. Baker, Newell Garfield,
Gary J. Massoth, Richard A. Feely, James P. Cowen,
Ronald R. Greene, Thomas A. Rago

The migration and evolution of a deep ocean hydrothermal event plume were tracked with a neutrally buoyant RAFOS float. The float remained entrained in the plume for 60 days, and the plume vorticity was calculated directly from the anticyclonic motion of the float. Concentrations of suspended particles, particulate iron, and dissolved manganese in the plume did not decay significantly during the 60 days, which indicates that event plumes would be easily detectable a year after formation.

In addition to the steady-state plumes produced by continuous hydrothermal venting, sea-floor hydrothermal systems also produce larger plumes that reside higher in the water column and are presumably caused by a cataclysmic release of hot water. The first of these event plumes was observed over the southern Juan de Fuca Ridge (JdFR) in 1986. It was an oblate spheroid ~20 km in diameter and 600 m thick, centered ~800 m above the sea floor, and with temperatures up to 0.25°C above that of the surrounding waters (*1*). This 1986 plume contained about 10^{17} J of excess heat, which is equivalent to the annual thermal output of a typical hydrothermal system. Modeling studies of this plume suggest that the hot water was released within a few hours (*2*). Although the exact origin of event plumes is unknown, event plume generation is somehow associated with the injection of magma into the ocean crust (*3–5*).

Large event plumes belong to a general class of subsurface circular eddies called "submesoscale coherent vortices" (SCVs) (*6*). Other SCVs such as Mediterranean salt lenses (meddies) or Gulf Stream rings (*6*) persist for months to years, which suggests that event plumes might have similar lifetimes in the ocean. The possibility of an extended lifetime for event plumes suggests that they may serve as floating oases rich in hydrothermal chemicals and biota, thereby aiding in the dispersal of both chemicals and larvae (*7*). The 1986 event plume over the JdFR was completely absent when the site was revisited 60 days later (*1*), and other event plumes have been similarly absent during subsequent visits to the original sites (*8, 9*). These observations seem to confirm the idea that event plumes are not maintained by steady-state hydrothermal input and suggest that the plumes may simply migrate off the ridge axis as discrete features. Theory and laboratory experiments indicate that a large ascending plume should have an anticyclonic rotation (clockwise in the Northern Hemisphere) because of the Coriolis force (*10–12*). The rotation curtails the lateral spread of the plume, thereby helping to preserve the plume as a coherent eddy. Thus, the dynamics and evolution of hydrothermal event plumes might be very similar to those of meddies, which are known to have long lifetimes in the open ocean (*13, 14*).

To test whether event plumes have extended lifetimes and to examine their dynamics in situ, we seeded an event plume with a RAFOS neutrally buoyant drifter (*15*). The event plume we tracked was generated on the Gorda Ridge (Fig. 1). The onset of the Gorda Ridge event was detected seismically in February 1996 (*16*). The seismic activity lasted about 3 weeks. The first response cruise to the site completed 14 vertical hydrocasts over the Gorda Ridge in March 1996 (*17*). Four of these casts detected strong hydrothermal event plumes at depths between 1900 and 2500 m, with temperatures up to 0.12°C above that of the surrounding waters (*9*). The plumes were enriched in ^{3}He, Mn, Fe, and other tracers (*18–22*). Baker (*9*) concluded that these water column anomalies corresponded to a single event plume (designated EP96A) that was still coalescing as it was being sampled. The EP96A plume was located near the *t*-phase event locations (*16*) and also near a new lava flow (*23*).

The second cruise in April 1996 [GREAT 2 (for Gorda Ridge Event Assessment Team) aboard the *R/V Wecoma*] detected several deep (~3000 m) steady-state–type plumes but failed to detect the core of the strong event plume observed a month earlier (*9*). However, a weaker plume in the same depth range of 1800 to 2400 m was detected over the top of the western wall of the Gorda axial valley. This plume, designated EP96B1, was smaller than EP96A and had a maximum temperature anomaly $\Delta\theta$ (*24*) of only ~0.02°C (Fig.

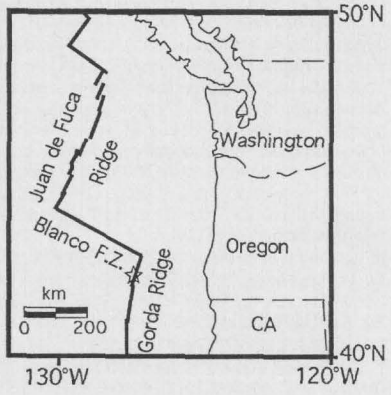

Fig. 1. Map showing the location of the Juan de Fuca and Gorda Ridges relative to the coast of Oregon and Washington. The star marks the location of the RAFOS float deployment.

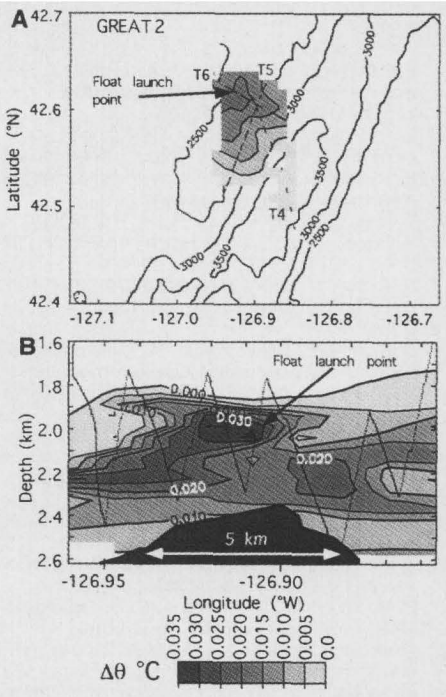

Fig. 2. Event plume EP96B1 discovered during the GREAT 2 cruise in April 1996. (**A**) Plan view map of temperature anomaly $\Delta\theta$. The contour interval for bathymetry is 500 m. Dashed lines are tow tracks of hydrographic tows T4, T5, and T6 conducted during GREAT 2. Bold arrow denotes the launch point of the RAFOS float. (**B**) Section view of temperature anomaly $\Delta\theta$ through event plume EP96B1 from GREAT 2 tow 6 [see (A) for location of tow track]. Dotted line denotes sawtooth track of towed sensor package.

J. E. Lupton and R. R. Greene, Pacific Marine Environmental Laboratory, National Oceanic and Atmospheric Administration (NOAA), Newport, OR 97365, USA.
E. T. Baker, G. J. Massoth, R. A. Feely, Pacific Marine Environmental Laboratory, NOAA, Seattle, WA 98115, USA.
N. Garfield and T. A. Rago, Naval Postgraduate School, Code OC/GF, Monterey, CA 93943, USA.
J. P. Cowen, Department of Oceanography, University of Hawaii, Honolulu, HI 96822, USA.

2) and a low ^{3}He/heat ratio [0.4×10^{-12} cm^3 at standard temperature and pressure (STP) per calorie] that is characteristic of event plumes (*25*). Based on the differing chemistry and total heat content of the two plumes (*19–22*), Baker (9) concluded that this second event plume (EP96B1) was not EP96A but a distinct plume perhaps generated in conjunction with a *t*-phase swarm recorded between March 10 and March 20 (*16*).

On 15 April 1996, the GREAT 2 team seeded the EP96B1 plume with a RAFOS float (NPS-37) ballasted to a depth of 2000 m. The float settled to a slightly greater depth of about 2200 m but still well within the plume envelope. The subsurface position of the RAFOS float is determined by means of moored sound sources (*26*). The RAFOS drifter uses a microprocessor in combination with an internal clock to record the arrival times of the sound signals. When the programmed mission length is reached, the float releases external ballast and ascends to the surface, where it transmits its recorded data to an orbiting ARGOS satellite. For our experiment, the float was programmed for a 56-day mission, so that it would surface at the beginning of the GREAT 3 expedition, which was scheduled to begin in June 1996. NPS-37 was programmed to record sound source arrivals twice daily.

The RAFOS drifter NPS-37 surfaced on 10 June 1996 at 42°44′N and 126°59′W, which was only 9 km from its launch point (Figs. 2 and 3). The *NOAA Ship Discoverer* proceeded to the site and found a large, symmetric event plume centered at 2200 m depth directly beneath the surfacing position of the float (Fig. 3). The plume, which we will refer to as EP96B2, was about 10 km in diameter and 0.5 km thick and had a maximum temperature anomaly $\Delta\theta$ = 0.065°C (9). The simplest interpretation of this result was that EP96B1 and EP96B2 were the same plume, and the float had remained entrained into the same event plume for about 2 months. However, EP96B2 had both a greater maximum temperature anomaly and higher concentrations of heat and chemicals than its predecessor EP96B1. One of the hydrographic tows conducted during GREAT 3 showed a trail of plume material from EP96B2 extending eastward from the plume core, which is remarkably similar to the weaker signals recorded for EP96B1 during GREAT 2 (9). This suggests that NPS-37 may have been launched into the disorganized edge of a larger plume that was not completely mapped during the GREAT 2 surveys.

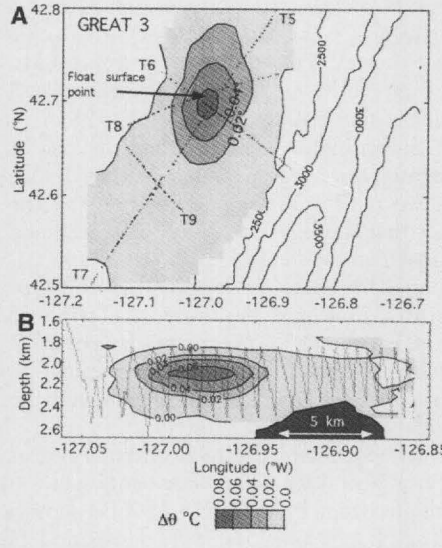

Fig. 3. Event plume EP96B2 discovered during the GREAT 3 cruise in June 1996. (**A**) Plan view map of temperature anomaly $\Delta\theta$. The contour interval for bathymetry is 500 m. Dashed lines are tracks of hydrographic tows T5 through T9. Bold arrow denotes the surfacing point of the RAFOS float. (**B**) Temperature anomaly $\Delta\theta$ contoured in section view through event plume EP96B2 from GREAT 3 tow 6 (see Fig. 3A for location of tow track). Dotted line denotes sawtooth track of towed sensor package.

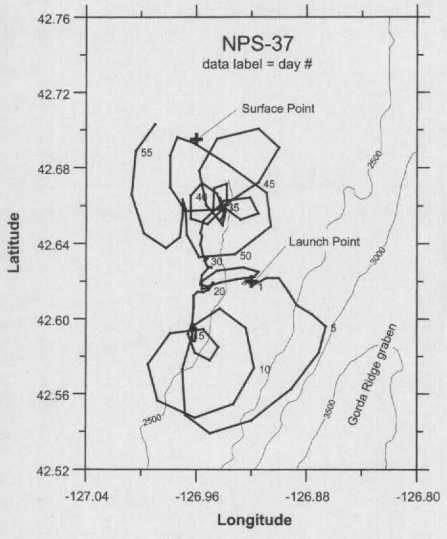

Fig. 4. Track of RAFOS float NPS-37 (bold lines). The position of the float was determined twice each day by recording the arrival times of signals from moored sound sources. The launch point and surfacing point of the float are marked with crosses. Labels denote the day number in 5-day increments during the 56-day mission. Thin lines are bathymetry contoured at a 500 m interval.

As shown in Fig. 4, the float track described several large anticyclonic circles with a mean diameter of 6.6 km. This is precisely the sense and approximate diameter of rotation expected for a float entrained into a circulating event plume in the Northern Hemisphere. The mean rotational period of the float was 8.5 days, the net velocity was ~0.4 cm s^{-1}, and its particle velocity averaged 2.4 cm s^{-1}. Although the float traveled a net distance of only 8.8 km, the total track length was 127 km.

The float motion was both rapid and periodic at the beginning and end of the mission; but during days 18 to 38, the average float speed dropped to ~1.2 cm s^{-1} as compared with the average of 2.4 cm s^{-1} for the entire float track. The anticyclonic motion seemed to disappear during this 20-day period. The core of each event plume should be in solid body rotation. Thus, this interval of low float speed may be due to migration of the float into the center of the event plume, where the float speed would be lower and the circular motion less pronounced.

During the first 18 days, the in situ temperature recorded by the float increased from

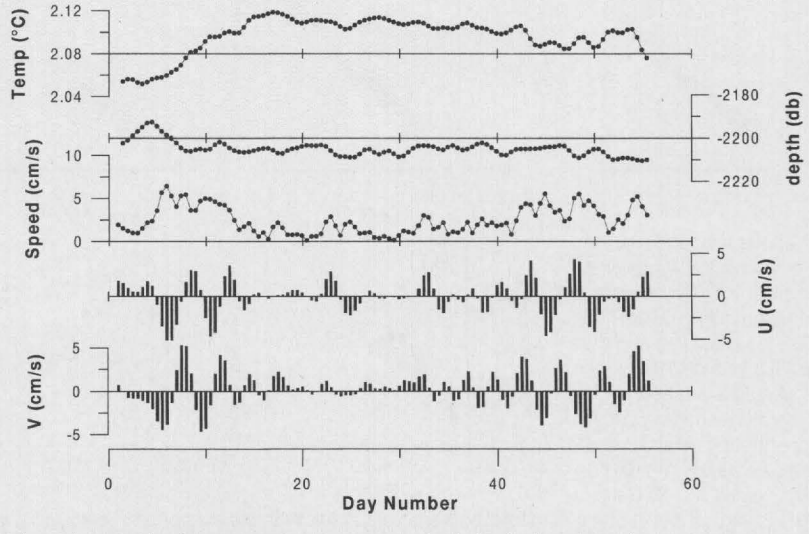

Fig. 5. Time history of in situ temperature, pressure depth (in decibars), total speed, east-west velocity component (U), and north-south velocity component (V) for RAFOS float NPS-37.

2.05° to 2.11°C as the speed and circular motion of the float slowly decreased (Fig. 5). This temperature increase (~0.06°C) is identical to the maximum temperature anomaly observed in the core of the event plume (Fig. 3). These observations also suggest that the float slowly migrated from the periphery of the event plume into the plume core.

For a coherent vortex in solid body rotation, the relative vorticity is simply twice the angular velocity (*27*). Assuming that the float rotational period of 8.6 days is a reliable indicator of the overall plume angular velocity, we calculate that the relative vorticity $\zeta = 8.45 \times 10^{-6}$ rad s^{-1} for EP96B1. This can also be expressed as $\zeta = -0.34f$, where $f = 2\Omega \times \sin\phi$, the planetary vorticity associated with a stationary water mass due to Earth's rotation (*28*). Our estimate for EP96B1 is comparable to previous vorticity estimates of $-0.5f$ and $-0.3f$ for the 1986 and 1987 megaplumes on the southern JdFR, based on the analysis of water column density structure (*6*). The event plumes are similar to other SCVs such as Gulf Stream eddies and meddies, which are 4 to 50 km in diameter and have relative vorticities of $-0.3f$ up to $-1.0f$ (*6*, *29*).

Assuming that EP96B1 and EP96B2 were the same plume observed at separate times, we can ask how this event plume evolved during that 60-day period. We have "before" and "after" pictures of the physical and chemical characteristics of the plume from the GREAT 2 and GREAT 3 expeditions. However, the plume signals were weaker during GREAT 2, as shown in Fig. 6. These differences are difficult to explain, because the intensity of plume signals should decrease rather than increase with time. However, as discussed above, we believe that the RAFOS float was launched into the edge of the event plume and that the hydrographic tows and casts conducted during GREAT 2 sampled the periphery of the plume and not the plume core. In contrast, the GREAT 3 expedition was able to collect samples from the center of the plume.

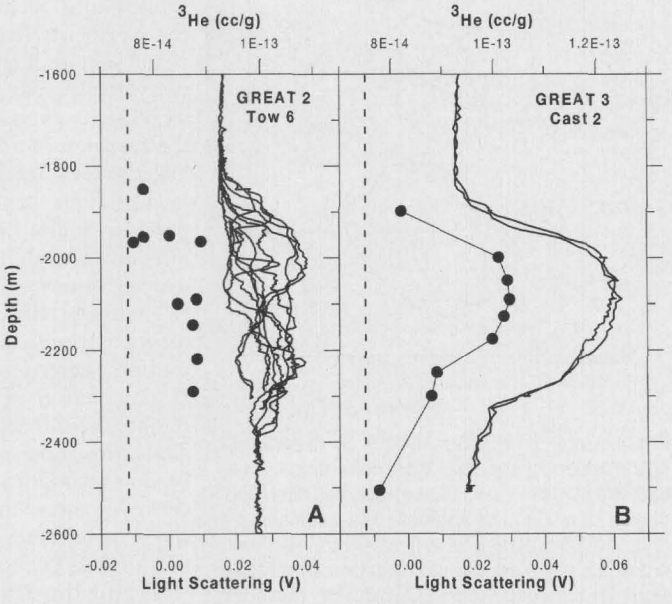

Fig. 6. Vertical profiles of ^{3}He (solid circles) and nephelometer light scattering (solid lines) versus depth through the event plumes EP96B1 and EP96B2. Samples were collected during (**A**) GREAT 2, tow 6, in April 1996 and (**B**) GREAT 3, cast 2, in June 1996. For the GREAT 2 expedition, no single profile through the event plume was available, therefore (A) shows a composite of several tow-yo passes through the plume.

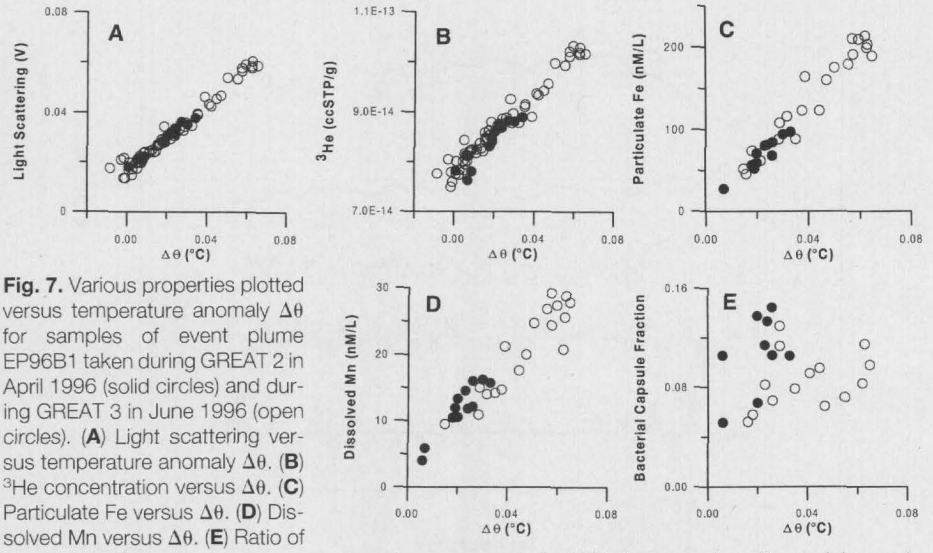

Fig. 7. Various properties plotted versus temperature anomaly Δθ for samples of event plume EP96B1 taken during GREAT 2 in April 1996 (solid circles) and during GREAT 3 in June 1996 (open circles). (**A**) Light scattering versus temperature anomaly Δθ. (**B**) ^{3}He concentration versus Δθ. (**C**) Particulate Fe versus Δθ. (**D**) Dissolved Mn versus Δθ. (**E**) Ratio of metal-depositing capsuled bacteria to total bacteria versus Δθ. With the exception of bacterial capsules (E), linear regression fits show that for each property pair there is no significant difference in the correlation for the GREAT 2 versus the GREAT 3 data within the errors of the measurements (*33*).

Because of this difference in the sampling of EP96B1 versus EP96B2, we studied the evolution of the plume by comparing ratios of properties to the temperature anomaly Δθ (in degrees centigrade), which is a conservative tracer unaffected by chemical or biological processes (Fig. 7). Of the other tracers, ^{3}He is conservative, whereas light-scattering particulate Fe and dissolved Mn are all nonconservative tracers that should evolve with time. The ratio of light scattering to Δθ should decrease with time as the suspended particle load is reduced by particle settling. For EP96B1, most of the Fe (~84%) was in the particulate phase, whereas most of the Mn (~95%) was dissolved (*20*, *21*). This distribution for Fe and Mn would be expected for a plume that is a few weeks old, because hydrothermal Fe is rapidly oxidized from the dissolved to an aggregated particulate phase on a time scale of ~ 1 week. The equivalent process for Mn is biologically mediated and proceeds on a time scale of weeks to years (*30*–*32*).

Surprisingly, the trends for the hydrothermal tracers show no measurable change between EP96B1 and EP96B2 (*33*). The fact that the light-scattering versus Δθ and particulate Fe versus Δθ trends are unchanged between EP96B1 and EP96B2 indicates that particles were not removed from the plume during the 60-day period of study. This result is additional confirmation that EP96B1 and EP96B2 are indeed the same plume.

In contrast to the hydrothermal tracers above, geomicrobial measurements made on samples from EP96B1 and EP96B2 show a clear change over the ~60-day period of study (Fig. 7E). Relative to temperature anomaly Δθ, metal-depositing bacteria were at a higher concentration in plume EP96B1 than in EP96B2. An opposite trend has been found in chronic plumes and in two unrelated event plumes on the southern JdFR (*34*). One explanation is that nonconservative conditions within the plume promote the rise and subsequent decay toward background of geomicrobial levels on a time

scale of less than 60 days (*22*).

Our data for EP96B1 and EP96B2 thus show that this event plume changed very slowly after it formed. In many plumes from the southern JdFR, light attenuation anomaly, assumed to be produced mainly by suspended particulate Fe, could be detected more than 20 km away from the source, indicating a long residence time for particulate Fe (*35*). Using radon as a clock, Kadko *et al.* (*32*) studied the removal rates of various hydrothermal constituents from the Endeavour Ridge effluent plume. They observed no measurable change in Mn concentrations with time and were only able to place a lower limit of $\tau \geq 20$ days for the residence time of total Mn (*36*). Our measurements indicate that light-scattering anomaly, particulate Fe, and dissolved Mn decreased by no more than 15% during the 60-day RAFOS experiment, indicating a residence time $\tau \geq 1$ year for these three hydrothermal tracers (*33*). For Fe, this estimate is similar to what has been found for steady-state plumes (*37*).

Future experiments might track an event plume for a year or more with several RAFOS floats programmed to surface at various stages in the plume evolution. Alternatively, floats equipped with acoustic transponders would allow surface ships to range on the floats, thereby eliminating the necessity of having the floats surface to locate the plume.

REFERENCES AND NOTES

1. E. T. Baker, G. J. Massoth, R. A. Feely, *Nature* **329**, 149 (1987).
2. J. W. Lavelle, *Geophys. Res. Lett.* **22**, 159 (1995).
3. R. W. Embley, W. W. Chadwick Jr., M. R. Perfit, E. T. Baker, *Geology* **19**, 771 (1991).
4. R. W. Embley, W. W. Chadwick Jr., I. R. Jonasson, D. A. Butterfield, E. T. Baker, *Geophys. Res. Lett.* **22**, 143 (1995).
5. R. W. Embley and W. W. Chadwick Jr., *J. Geophys. Res.* **99**, 4741 (1994).
6. E. D'Asaro, S. Walker, E. T. Baker, *ibid.*, p. 20361.
7. L. S. Mullineaux and S. C. France, in *Seafloor Hydrothermal Systems: Physical, Chemical, Biological, and Geological Interactions*, S. E. Humphris, R. A. Zierenberg, L. S. Mullineaux, R. E. Thomson, Eds. [American Geophysical Union (AGU), Washington, DC, 1995], pp. 408–424; L. S. Mullineaux, P. H. Wiebe, E. T. Baker, *Oceanus* **34**, 64 (1991).
8. E. T. Baker *et al.*, *Geophys. Res. Lett.* **22**, 147 (1995).
9. E. T. Baker, in preparation.
10. K. G. Speer, *Geophys. Res. Lett.* **16**, 461 (1989).
11. K. R. Helfrich and K. G. Speer, in *Seafloor Hydrothermal Systems: Physical, Chemical, Biological, and Geological Interactions*, S. E. Humphris, R. A. Zierenberg, L. S. Mullineaux, R. E. Thomson, Eds. (AGU, Washington, DC, 1995), pp. 347–356.
12. K. R. Helfrich and T. M. Battisti, *J. Geophys. Res.* **96**, 12511 (1991).
13. J. C. McWilliams, *Rev. Geophys.* **23**, 165 (1985).
14. L. Armi *et al.*, *J. Phys. Oceanogr.* **19**, 354 (1989).
15. RAFOS is not an acronym but is SOFAR spelled backward. SOFAR (Sound Fixing and Ranging) floats emit sounds that are detected by fixed hydrophones, which is the opposite of the method of the RAFOS floats.
16. C. G. Fox and R. P. Dziak, in preparation.
17. Three different response cruises documented the effects of the 1996 Gorda Ridge event on the ocean water column and sea floor. These expeditions are now referred to as GREAT 1, 2, and 3, after the Gorda Ridge Event Assessment Team.
18. J. E. Lupton, unpublished data.
19. D. S. Kelley, M. D. Lilley, J. E. Lupton, E. J. Olson, *Deep-Sea Res.*, in press.
20. R. Feely *et al.*, *ibid.*, in press.
21. G. J. Massoth *et al.*, *ibid.*, in press.
22. J. P. Cowen *et al.*, *ibid.*, in press.
23. W. W. Chadwick Jr. and R. W. Embley, in preparation.
24. The apparent excess heat is reported in the form of temperature anomaly $\Delta\theta$, which is the deviation of the potential temperature θ from the ambient θ versus potential density (σ_θ) relation, which is linear for the deep waters of the northeast Pacific. Thus, $\Delta\theta = \theta - k\sigma_\theta - b$, where k and b are, respectively, the empirically determined slope and intercept of the θ versus σ_θ line.
25. J. E. Lupton, E. Baker, G. Massoth, *Nature* **337**, 161 (1985); J. E. Lupton *et al.*, *Geophys. Res. Lett.* **22**, 155 (1995).
26. H. T. Rossby, D. Dorson, J. Fontaine, *J. Atmos. Ocean. Tech.* **3**, 672 (1986).
27. S. Pond and G. L. Pickard, *Introductory Dynamic Oceanography* (Pergamon, Oxford, UK, 1978), p. 120.
28. Here $\Omega = 7.29 \times 10^{-5}$ rad s^{-1}, the angular velocity of Earth's rotation, and ϕ = latitude. The minus sign for the relative vorticity of the event plumes indicates an anticyclonic sense of rotation.
29. For event plume EP96B2, we calculate the internal Rossby radius to be ~30 km, which is considerably larger than the radius of the plume itself, which was ~5 km. Thus, the event plume was a submesoscale feature.
30. G. J. Massoth *et al.*, *J. Geophys. Res.* **99**, 4905 (1994).
31. J. W. Lavelle, J. P. Cowen, G. J. Massoth, *ibid.* **97**, 7413 (1992); C. S. Chin *et al.*, *ibid.* **99**, 4969 (1994).
32. D. C. Kadko, N. D. Rosenberg, J. E. Lupton, R. C. Collier, M. D. Lilley, *Earth Planet. Sci. Lett.* **99**, 315 (1990).
33. We quantified changes in light scattering, ^{3}He concentration, particulate Fe, and dissolved Mn between EP96B1 and EP96B2 by means of separate linear regression fits to each of these properties versus $\Delta\theta$ (Fig. 7). In each case, the linear regression fits gave slopes for EP96B1 and EP96B2 that agreed within one standard deviation. The slopes for EP96B1 and EP96B2 differed at most by 15%, a difference we attribute to measurement errors. This 15% difference is the basis for lower limit caiculated for the residence time of these properties.
34. J. P. Cowen and Y. H. Li, *J. Mar. Res.* **49**, 517 (1991); J. F. Gendron, J. P. Cowen, R. A. Feely, E. T. Baker, *Deep-Sea Res. I* **40**, 1559 (1993).
35. E. T. Baker and G. J. Massoth, *Earth Planet Sci. Lett.* **85**, 59 (1987).
36. The residence time τ is defined as the time for the concentration to be reduced to 1/e or 0.368 of its original value, assuming that the concentration of property X decays exponentially as $X(t) = X_0 e^{-t/\tau}$.
37. R. A. Feely *et al.*, *Geochim. Cosmochim. Acta* **60**, 2297 (1996).

38. We thank G. Lebon, J. Gendron, S. Maenner, J. Resing, E. Olson, X. Wen, D. Tennant, and the officers and crews of the *NOAA Ship MacArthur*, the *R/V Wecoma*, and the *NOAA Ship Discoverer* for assistance with the sample collections at sea; S. Walker for assistance in the collection and analysis of the hydrographic data; and L. Evans, G. Lebon, J. Gendron, S. Maenner, and X. Wen for the analysis of water samples. J. Waddell provided valuable editorial assistance. The paper profited from discussions with C. Collins and G. Cannon and from reviews by two anonymous reviewers. This research was funded by the NOAA VENTS Program, by NSF grant OCE93-20240 to the Monterey Naval Postgraduate School, and by NSF grant OCE96-34637 to the University of Hawaii. This is Pacific Marine Environmental Laboratory contribut on number 1932.

21 January 1998; accepted 17 March 1998

Earthquakes on Dipping Faults: The Effects of Broken Symmetry

David D. Oglesby, Ralph J. Archuleta,* Stefan B. Nielsen

Dynamic simulations of earthquakes on dipping faults show asymmetric near-source ground motion caused by the asymmetric geometry of such faults. The ground motion from a thrust or reverse fault is larger than that of a normal fault by a factor of 2 or more, given identical initial stress magnitudes. The motion of the hanging wall is larger than that of the footwall in both thrust (reverse) and normal earthquakes. The asymmetry between normal and thrust (reverse) faults results from time-dependent normal stress caused by the interaction of the earthquake-generated stress field with Earth's free surface. The asymmetry between hanging wall and footwall results from the asymmetric mass and geometry on the two sides of the fault.

Historically, much earthquake research in the United States has focused on large vertical strike-slip faults such as the San Andreas Fault in California. However, for compressive tectonic regimes such as the Los Angeles area, Japan, and Central and South America, and in extensional regimes such as the Mediterranean and the Great Basin of Nevada, Utah, and Idaho, seismic hazard lies in nonvertical (dipping) faults (*1*). One difference between a vertical and a nonvertical fault is the breakdown of symmetry with respect to the free surface in the nonvertical case (Fig. 1). Because of this geometrical asymmetry, the earthquake-generated stress field must change to match

D. D. Oglesby and R. J. Archuleta, Institute for Crustal Studies and Department of Geological Sciences, University of California at Santa Barbara, Santa Barbara, CA 93106, USA.
S. B. Nielsen, Institute for Crustal Studies and Materials Research Laboratory, University of California at Santa Barbara, Santa Barbara, CA 93106, USA.

*To whom correspondence should be addressed.